Extended Abstracts of the 2009 International Conference on Solid State Devices and Materials, Sendai, 2009, pp1138-1139

Random Telegraph Signal and Low Frequency Noise in Silicon Charge-Sensitive Electrometers

Nicolas Clement[1], Katsuhiko Nishiguchi[2], Akira Fujiwara[2] and Dominique Vuillaume[1]

[1]CNRS, Institute for Electronics, Microelectronics and Nanotechnology
Cite Scientifique, avenue Poincare, Villeneuve d'Ascq 59652, France
Phone: +33-3-20-19-79-32 E-mail: nicolas.clement@iemn.univ-lille1.fr
[2]NTT Basic Research Laboratories, NTT Corporation,
3-1 Morinosato- Wakamiya, Atsugi, Kanagawa 243-0198, Japan

1. Introduction

Random telegraph signal (RTS) in small area transistors – discrete switching in the current between two or more levels under constant bias conditions – has been a favored tool in the study of individual traps and their impact on low frequency noise [1]. Interestingly in our device, due to Coulomb repulsion, traps are active one by one as the back-gate voltage is scanned. Thanks to the well suited architecture of this electrometer usually used for single electron memories [2], a perfect consistency on RTS amplitude for all traps is observed. We discuss on RTS noise theories, include drain voltage dependence and extract quantitative parameters such as capacitances and scattering constants. Finally, at the light of these results, appropriate biases for remote electron sensing are proposed.

2. Experimental details and results

A schematic view of the silicon MOSFET device with silicon constriction part (width W=30 nm, length L=60 nm) fabricated by e-beam lithography is shown in Fig.1a. Source is grounded, drain voltage Vd is first set to 50 mV and Vbg is sweept from the "off" to "on" state of the transistor. When an electron transits back/forth between the channel and the trap through the tunnel barrier Cj, RTS can be observed. Typical RTS measured at room temperature and current histogram, are shown in Fig.1b. Up and down times follow poissonian distribution. If one neglects for a moment the possible impact on the mobility, RTS amplitude ΔI should follow eq.1, which is also used for single electron memories [2,3].

$$\frac{\Delta I}{gm} = \frac{e}{Cg} \qquad (1)$$

where e is the electron charge and gm the transconductance.

A wide spread of RTS amplitudes is usually observed, mainly because the oxide thickness is not large compared to trap depth (fluctuation of Cg) and because the device dimensions (in particular the width) are larger than the Debye screening length (70 nm for SiO_2 [3]). Here it is the opposite (W=30 nm and oxide thickness = 400 nm). Fig.2 shows I-V, ΔI-V for the 5 traps (left side) and gm-V (right side). One can clearly see that ΔI follows gm. Using eq.1, Cg can be estimated (Fig.3). Under the flat band voltage, Cg is constant. Its value (0.91 aF +/- 20%) gives a good estimation of the gate oxide capacitance Cox ≈ Cg, which is difficult to measure by other techniques in the aF range. Over the flat band voltage, Cg increases. This reflects the necessity to include a mobility fluctuation term due to trap scattering [4] and evidences that these traps are positively charged when empty. One can rewrite eq (1) as:

$$\frac{\Delta I}{gm} = \frac{e\left(1 - \frac{\alpha_{sc}\mu Cox}{eWL}(Vbg - Vfb)\right)}{Cg} \qquad (2)$$

where $\alpha_{sc} \approx 7.7\text{x}10^{-15}$ V.s is a scattering parameter in the same order of magnitude than in ref [4] (taken as 0 if $Vbg < Vfb$), $\mu \approx 35$ cm^2/Vs is the mobility at low electric field, $Cox \approx 9.1\text{x}10^{-19}$ F the gate capacitance, $Vfb \approx 13$ V the flat-band voltage.

This equation is the basis of low frequency noise in our devices and can be confirmed by plotting $\Delta I/I$ curves (Fig.4). In the subthreshold region, $\Delta I/I$ is constant, inversely proportional to C_Σ, where C_Σ=S.Cg.e/(kT.ln10) and S is the subthreshold swing, k the Boltzmann constant, T the temperature. Normalized current is also plotted with drain dependence (Fig.4 inset). It shows a linear decrease with drain voltage probably related to mobility fluctuation. Since traps are basically active one by one, a simple expression for power spectrum noise can be derived.

Finally, the trap occupancy function is plotted in Fig.5. For traps 1 to 4, we can note that one is almost filled when the next one start being active.

3. Conclusions

We have studied the RTS noise amplitude at room temperature on one of the simplest systems i.e. very low density of traps, Debye screening length > devices dimensions and traps depth negligible compared to oxide thickness (ratio > 200 here). Due to Coulomb repulsion, traps are active one by one. This allows us to confirm the validity of the correlated number/mobility fluctuation model and include drain bias dependence. Gate capacitance in the aF range can be precisely estimated (+/- 20 %), which is difficult from other techniques. Tunnel capacitance $Cj \approx 54$ aF can be estimated from the trap occupancy function and is the main parasitic capacitance. Finally we conclude that, for our devices, strong accumulation can be well suited for remote electron sensing because of the relative reduction of

RTS amplitude due to correlated mobility fluctuation. Increased drain voltage, also reduces RTS relative amplitude. Some of the devices show no RTS and much lower power spectrum current noise meaning that no trap is located to electrometer proximity.

References

[1] M.J. Uren and M.J. Kirton, Adv. Phys. **33** (1989) 367; N.Clement, Y.Ono & H.Inokawa Jpn.J.Appl.Phys **45** (2006) 3606

[2] K. Nishiguchi, H. Inokawa, Y. Ono, A. Fujiwara and Y. Takahashi Appl.Phys.Lett. 85 (2004) 1277

[3] L. Guo, E. Leobandung and S.Y. Chou Science 275 (1997) 649

[4] K.K. Hung, P.K. Ko, C. Hu, Y.C. Cheng IEEE Electron Device Lett. 11 (1990) 90

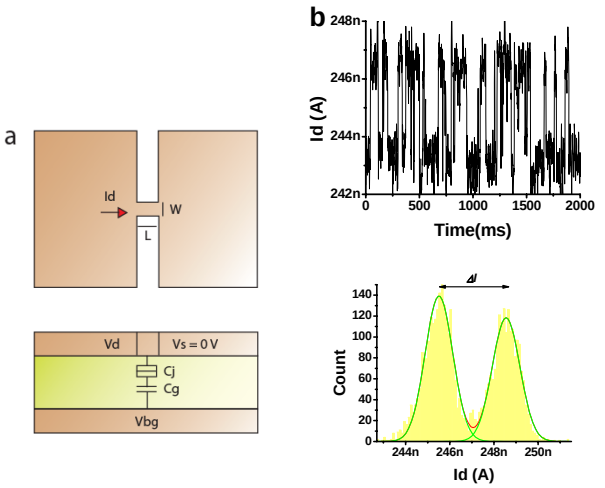

Fig. 1a: Top and side views of the SOI device with a constriction part of dimensions *W*=30 nm and *L*=60 nm. 1b: typical RTS observed at *Vd*=50 mV and drain current histogram.

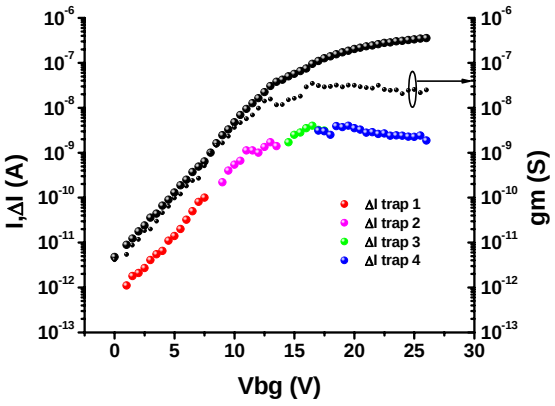

Fig. 2: *Id-Vbg* and its derivative *gm-Vbg* curves are plotted with large and small black balls respectively. *ΔI-Vbg* curves (colored balls) for 5 different traps follow almost *gm-Vbg*.

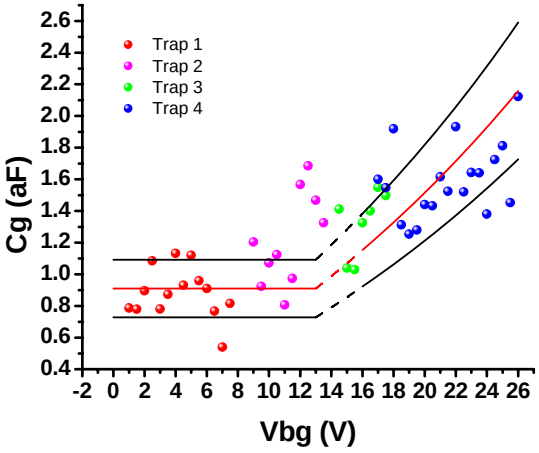

Fig.3 *Cg-Vbg* with *Cg* obtained from eq.1. These results allow an improvement of the model to eq.2.

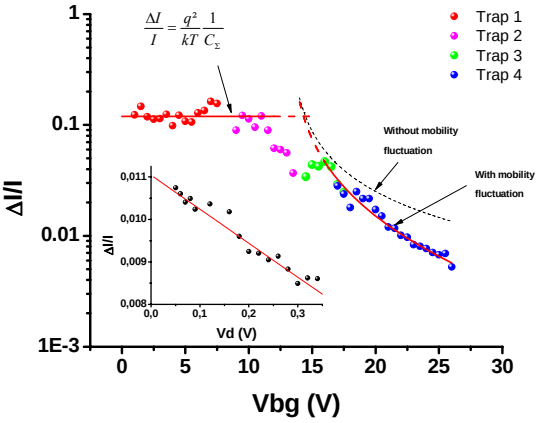

Fig.4 *ΔI/I* experimental datas (balls) and the theoretical curve in agreement with eq.2. Inset, *ΔI/I* vs *Vd*.

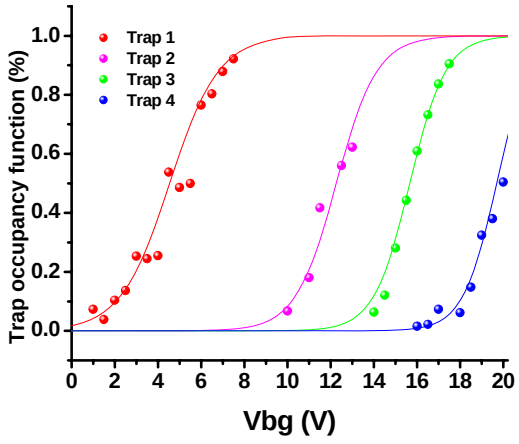

Fig.5 Trap occupancy function $\tau_e/(\tau_e+\tau_c)$ where τ_e and τ_c are emission and capture average times of the trap, respectively.